Therapeutic Effects of a Novel Agonist of Peroxisome Proliferator-Activated Receptor Alpha for the Treatment of Diabetic Retinopathy

Guotao Deng,[1,2] Elizabeth P. Moran,[2] Rui Cheng,[2] Greg Matlock,[2] Kelu Zhou,[2] David Moran,[2] Danyang Chen,[2] Qiang Yu,[1] and Jian-Xing Ma[2]

[1]State Key Laboratory of Ophthalmology, Zhongshan Ophthalmic Center, Sun Yat-sen University, Guangzhou, China
[2]Department of Physiology, University of Oklahoma Health Sciences Center, Oklahoma City, Oklahoma, United States

Correspondence: Jian-Xing Ma, Department of Physiology, University of Oklahoma Health Sciences Center, 941 Stanton L. Young Boulevard, Oklahoma City, OK 73104, USA; jian-xing-ma@ouhsc.edu.

Submitted: December 30, 2016
Accepted: August 22, 2017

Citation: Deng G, Moran EP, Cheng R, et al. Therapeutic effects of a novel agonist of peroxisome proliferator-activated receptor alpha for the treatment of diabetic retinopathy. *Invest Ophthalmol Vis Sci*. 2017;58:5030–5042. DOI:10.1167/iovs.16-21402

Purpose. Clinical studies have shown that peroxisome proliferator-activated receptor alpha (PPARα) agonist fenofibrate has therapeutic effects on diabetic retinopathy (DR). The purpose of this study was to identify a novel PPARα agonist and to evaluate its beneficial effects on DR.

Methods. The transcriptional activity of PPARα was measured by a luciferase-based promoter assay. TUNEL was used to evaluate apoptosis in retinal precursor cells (R28). Diabetes was induced in rats by injection of streptozotocin. Retinal inflammation was examined using leukostasis assay, and retinal vascular leakage was measured using permeability assay. Retinal function was measured using electroretinogram (ERG) recording, and retinal apoptosis was quantified using the cell death ELISA. The anti-angiogenic effect was evaluated in the oxygen-induced retinopathy (OIR) model.

Results. A compound, 7-chloro-8-methyl-2-phenylquinoline-4-carboxylic acid (Y-0452), with a chemical structure distinct from existing PPARα agonists, activated PPARα transcriptional activity and upregulated PPARα expression. Y-0452 significantly inhibited human retinal capillary endothelial cell migration and tube formation. The compound also protected R28 cells against apoptosis and inhibited NF-κB signaling in R28 cells exposed to palmitate. In diabetic rats, Y-0452 ameliorated leukostasis and vascular leakage in the retina. In addition, Y-0452 preserved the retinal function and reduced retinal cell death in diabetic rats. Y-0452 also alleviated retinal neovascularization in the OIR model.

Conclusions. Y-0452 is a novel PPARα agonist and has therapeutic potential for DR.

Keywords: inflammation, apoptosis, agonist, PPARα, angiogenesis, diabetic retinopathy

Diabetic retinopathy (DR) is a common complication of diabetes and a leading cause of blindness in developed countries.[1] Previous studies suggest that DR is a chronic inflammatory disorder, as multiple inflammatory factors, such as TNF-α, intercellular adhesion molecule-1 (ICAM-1), and VEGF, are overexpressed in the diabetic retina.[2–5] Retinal apoptosis also plays an important part in the development of DR, especially apoptosis of vascular cells and neurons in the retina.[6–9] It is important to develop new drugs with anti-inflammatory and antiapoptotic effects for the treatment of DR.

Two prospective clinical studies (FIELD and ACCORD) have demonstrated that fenofibrate, a specific agonist of peroxisome proliferator-activated receptor alpha (PPARα), has robust therapeutic effects on DR in patients with type 2 diabetes.[10,11] In recent years, studies have focused on the roles of PPARs in ischemic retinopathy.[3,12–15] Our previous studies have shown that diabetes-induced downregulation of PPARα in the retina plays a major role in the pathogenesis of DR.[3] PPARα has antioxidant and anti-inflammatory effects in some disease models, such as Alzheimer's disease, DR, diabetic neuropathy, traumatic brain injury, and stroke.[16–19] PPARα also exerts protective effects against endothelial dysfunction, pathological neovascularization, vasoregression, and vascular hyperpermeability.[20–23] Taken together, these studies demonstrated that PPARα is a potential therapeutic target for DR.

It is desired to develop new PPARα agonists effective on those DR patients who do not respond to fenofibrate. New PPARα agonists with binding sites on PPARα different from fenofibrate may be applied in combination with fenofibrate to improve efficacy. Further, new PPARα agonists with chemical structures different from fenofibrate may avoid off-target side effects of fenofibrate. Therefore, the present study examined some compounds for their PPARα agonist activities, among which, 7-chloro-8-methyl-2-phenylquinoline-4-carboxylic acid (Y-0452, molecular weight [MW]: 297, Fig. 1A) was identified as a novel PPARα agonist with a structure distinct from existing PPARα agonists. We have demonstrated its effect on retinal endothelial dysfunction, angiogenesis, and inflammation, suggesting that it might be a novel drug candidate for DR.

Methods

Drugs and Chemicals

The compound 7-chloro-8-methyl-2-phenylquinoline-4-carboxylic acid, also named Y-0452, was originally identified from a compound library of the National Cancer Institute using

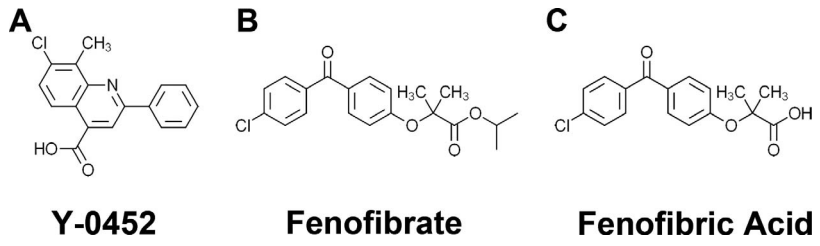

FIGURE 1. Chemical structures of Y-0452 (MW: 297), 7-chloro-8-methyl -2-phenylquinoline-4-carboxylic acid (**A**), fenofibrate (**B**) and fenofibric acid (**C**).

protein docking simulation software. The compound was obtained from the National Cancer Institute for the luciferase assay to confirm its activity as a PPARα agonist. Y-0452 was later purchased from Aurum Pharmatech LLC (Howell, NJ, USA). Fenofibric acid (Feno-FA) was purchased from Sigma-Aldrich Corp. (St. Louis, MO, USA). The chemical structures of these compounds are shown in Figure 1.

Cell Lines

R28, a cell line derived from photoreceptor precursors, a kind gift from Dr. Gail Seigel, were cultured in Dulbecco's modified Eagle's medium (DMEM) supplemented with 10% fetal bovine serum (FBS; Cellgro, Manassas, VA, USA) and 1% antibiotic-antimycotic solution (Cellgro).[24] Primary human retinal capillary endothelial cells (HRCECs), were purchased from Cell Systems Corporation (Kirkland, WA, USA) and cultured in endothelial basal growth medium (Lonza, Walkersville, MD, USA) with 20% FBS and 50 U/mL endothelial cell growth factor (Lonza), and 1% insulin-transferrin-selenium. All cells used in experiments were grown at 37°C in an atmosphere of 5% CO_2.

Animals

Brown Norway (BN) rats were purchased from Charles River Laboratories (Wilmington, MA, USA), *PPARα*$^{-/-}$ mice and age-matched C57/BL6J mice (wild-type [WT]) were purchased from Jackson Laboratories (Bar Harbor, ME, USA). Care, use, and treatment of experimental animals were in agreement with the ARVO Statement for the Use of Animals in Ophthalmic and Vision Research and approved by the Institutional Animal Care and Use Committee of The University of Oklahoma Health Sciences Center.

Streptozotocin (STZ)-induced Diabetes

Experimental diabetes was induced by an intraperitoneal injection of STZ (50 mg/kg) into 8-week-old BN rats after fasting overnight. Blood glucose levels were measured 48 hours after STZ injection and monitored monthly after that. Only animals with glucose levels >350 mg/dL were considered diabetic. No insulin was administered.

Oxygen-induced Retinopathy (OIR)

The OIR animal model was induced in mice according to a documented protocol with minor modifications.[25] Briefly, WT or *PPARα*$^{-/-}$ pups at postnatal day 7 (P7) with their mothers were exposed to hyperoxia (75% O_2) for 5 days (P7–P12) and returned to room air at P12. The animals were randomly divided into three groups: normoxia, OIR + vehicle, OIR + Y-0452. OIR pups were separately injected with the same volume of vehicle (DMSO) and Y-0452 (10 mg/kg/d) (intraperitoneally, 10 mg/kg/d) after return to normoxia (P12–P16). In the normoxia group, newborn pups were placed in constant room air from P0 to P17 and injected with vehicle control from P12 to P16. Animals were euthanized at P17 and perfused with prewarmed (37°C) PBS, and retinas were then homogenized in radioimmunoprecipitation assay lysis buffer for Western blotting. Other pups were subjected to retinal lectin staining and retinal vascular leukostasis assay. Pups that weighed less than 4 g at P17 were excluded from the study.

TUNEL Assay

R28 cells at 75% confluency were treated with different concentrations of Y-0452 and Feno-FA, or vehicle (DMSO) for 4 hours, and then co-incubated with 200 μM palmitate for another 24 hours. DNA fragments were labeled using the In Situ Cell Death Detection TMR red kit (Roche Diagnostics Corp., Indianapolis, IN, USA) following the manufacturer's instructions. Cells were mounted with antifade reagent containing 4′,6-diamidino-2-phenylindole (DAPI; Vector Laboratories, Inc., Burlingame, CA, USA). Images were captured under an inverted fluorescence microscope (Olympus, Tokyo, Japan).

Retinal Endothelial Cell Tube Formation

HRCECs at passage five were used in this study. For tube formation assay, 48-well plates were coated with 100 μL ice-cold Matrigel (BD Biosciences, San Jose, CA, USA), which was solidified by incubation at 37°C for 30 minutes. HRCECs were trypsinized and resuspended to 5×10^4/mL in the indicated concentration of the vehicle or compounds, then the suspended cells were seeded into each well, and incubated at 37°C for 6 hours. After incubation, photographs of tube formation from five random fields of each well were captured under a phase-contrast microscope. The branching points of the tubular structures were counted for analysis.

Endothelial Cell Scratch Wound-Healing Assay

HRCECs at 100% confluence in six-well plates were scratched using a sterile pipette tip to make a straight line across the cell monolayer. Then the cells were incubated with different concentrations of indicated chemicals for 24 hours. Photographs were captured at 0 and 24 hours after the scratch under a microscope. The average linear migration distance of the cells was calculated by measuring the distance of the wound monolayer and the cell migration distance by an investigator masked to cell treatment.

Luciferase Reporter Assay

Cells from the PPAR Response Element (PPRE) Luciferase reporter/PPARα expressing Combo cell line (PrimCells, LLC, San Diego, CA, USA) were seeded into 24-well plates at 2×10^5 cells per well in DMEM plus 10% FBS and 1 μg/mL doxycycline (to induce PPARα expression). After 24 hours, the cells were

Investigative Ophthalmology & Visual Science

treated with DMSO (control) and Y-0452 for 36 hours. The cells were lysed with 100 μL lysis buffer. Firefly luciferase activity was measured using the Dual-Luciferase Reporter Assay System (Promega, Madison, WI, USA) according to the manufacturer's instructions.

Retinal Cell Death ELISA

Retinal DNA cleavage was quantified using an ELISA kit (Cell Death Detection ELISA; Roche Diagnostics Corp.) and normalized to retinal wet weight as documented previously with minor modifications.[26] Briefly, the retinas were isolated immediately, and placed into a tube with lysis buffer (200 μL per retina) and wet weight recorded. Retinal tissues were homogenized using a plastic homogenizer. Each sample was vortexed for 5 seconds and incubated for 30 minutes with gentle rocking. The samples were then centrifuged at 10,000*g*, 4°C for 10 minutes, and 100 μL supernatant was collected. For each retinal sample, 20 μL supernatant was transferred into an ELISA plate. The colorimetric values were measured at 405 nm using a plate reader (reference wavelength 490 nm). DNA fragmentation of each retina was expressed as optical density normalized by retinal wet weight.

Retinal Vascular Permeability Assay

Retinal vascular permeability was quantified using Evans blue as a tracer according to a documented method.[27] Briefly, rats were anesthetized, and Evans blue (30 mg/mL, 1 μL/g body weight; Sigma-Aldrich, Hamburg, Germany) was injected through the iliac vein. At 2 hours after injection of the dye, the rats were perfused via the left ventricle with prewarmed (37°C) citrate buffer (50 mmol/L, pH 3.5). The retina was dissected, and Evans blue dye was extracted using formamide. Absorbance was measured at 620 nm with a spectrophotometer (DU800; Beckman Coulter, Brea, CA, USA). Concentration of Evans blue in the retina was calculated from a standard curve of Evans blue in formamide and normalized by protein concentrations as measured using the BCA assay kit (Pierce, Rockford, IL, USA). Retinal vascular permeability was expressed as micrograms of Evans blue per milligram of retinal protein.

Retinal Vascular Leukostasis Assay

The leukostasis assay was performed as described in a documented procedure, with minor modifications.[28] Briefly, mice or rats were deeply anesthetized. The chest cavity was carefully opened, the descending aorta was clamped, and a 14-guage perfusion canula was inserted into the left ventricle. The right atrium was cut open immediately before perfusion. The mice or rats were perfused with warm PBS to remove nonadherent leukocytes. FITC-conjugated concanavalin A (conA) (200 μg/mL in PBS, pH 7.4, 5 mg/kg body weight; Vector Laboratories) was then perfused to label adherent leukocytes and vascular endothelial cells. Animals were then perfused with PBS to remove the unbound conA. The eyes were removed and fixed in 4% paraformaldehyde for more than 1 hour. Then the retinas were flat mounted, and the adherent leukocytes were counted under a fluorescence microscope.

TUNEL and Immunohistochemistry in OIR Mouse Retinas

TUNEL and immunohistochemistry of OIR retinas were performed following a documented method.[29] Briefly, eyeballs were fixed in 4% paraformaldehyde for 1 hour and eyecups were incubated in 30% sucrose overnight, followed by optimal cutting temperature media (Sakura Finetek, Inc., Torrance, CA, USA) for snap freezing. Eyecups were sectioned at 10 μm. TUNEL-positive cells in the retina were detected by ATMR Red TUNEL kit (Roche Diagnostics Corp.) according to the manufacturer's instructions and then stained with DAPI (Vector Laboratories). Six cross sections from each sample were used in TUNEL analyses. For colabeling CD31 (Santa Cruz Biotechnology, Inc., Santa Cruz, CA, USA), sections were first labeled with TUNEL as described above and then immunostained with an antibody for CD31. Colabeling studies were performed on in least three different animals per group.

Quantification of Retinal Neovascularization and Vaso-obliteration in OIR Mice

The eyes were enucleated at P17 and fixed with 4% paraformaldehyde for 2 hours. The retinas were dissected and stained overnight with *Griffonia bandereiraea simplicifolia* Isolectin B4 (Cat. I21413, 1:100 dilution; Molecular Probes, Carlsbad, CA, USA) in 1 mM $CaCl_2$ in PBS. After washes for 2 hours with PBS, the retinas were whole-mounted onto microscope slides. Retinal images were captured under a fluorescence microscope. Retinal neovascularization and vaso-obliteration areas were quantified using Adobe Photoshop software (Adobe Systems, Inc., San Jose, CA, USA) as described in a previous study.[30]

ERG Recording

ERG was recorded using the Diagnosys Espion Visual Electrophysiology System (Lowell, MA, USA). Rats were anesthetized, and the pupils dilated with 1% Atropine. For scotopic ERG, rats were dark-adapted for 16 hours. For photopic ERG, light adaptation was 7 minutes. The flash intensities was 1000 cd·s/m^2 for scotopic ERG and 2000 cd·s/m^2 for photopic ERG. The ERG response of both eyes were simultaneously recorded and analyzed.

Western Blot Analysis

Thirty micrograms of proteins from each sample were resolved by SDS-PAGE and transferred onto nitrocellulose membranes. Primary antibodies used were anti–nuclear factor (NF)-κB (Cell Signaling, Danvers, MA, USA), anti-phospho-NF-κB (Cell Signaling), anti-IκBα (Cell Signaling), anti-PPARα (Abcam, Cambridge, MA, USA), anti-PPARβ (Santa Cruz Biotechnology, Inc.), anti-PPARγ (Santa Cruz Biotechnology, Inc.), anti-VEGF (Santa Cruz Biotechnology, Inc.), anti-TNF-α (Abcam), and anti-β-actin (Abcam). Primary antibodies were then detected with HRP-conjugated secondary antibodies, and signals developed using ECL plus (Amersham GE Healthcare, Marlborough, MA, USA) detection kit. Results were semiquantified using Image J software (http://imagej.nih.gov/ij/; provided in the public domain by the National Institutes of Health, Bethesda, MD, USA).

Statistical Analysis

Data were expressed as mean ± SD. Statistical differences between groups were analyzed using Student's *t*-test for two groups, and 1-way or 2-way ANOVA with Bonferroni's post hoc test for three or more groups. $P \leq 0.05$ was considered statistically significant.

Investigative Ophthalmology & Visual Science

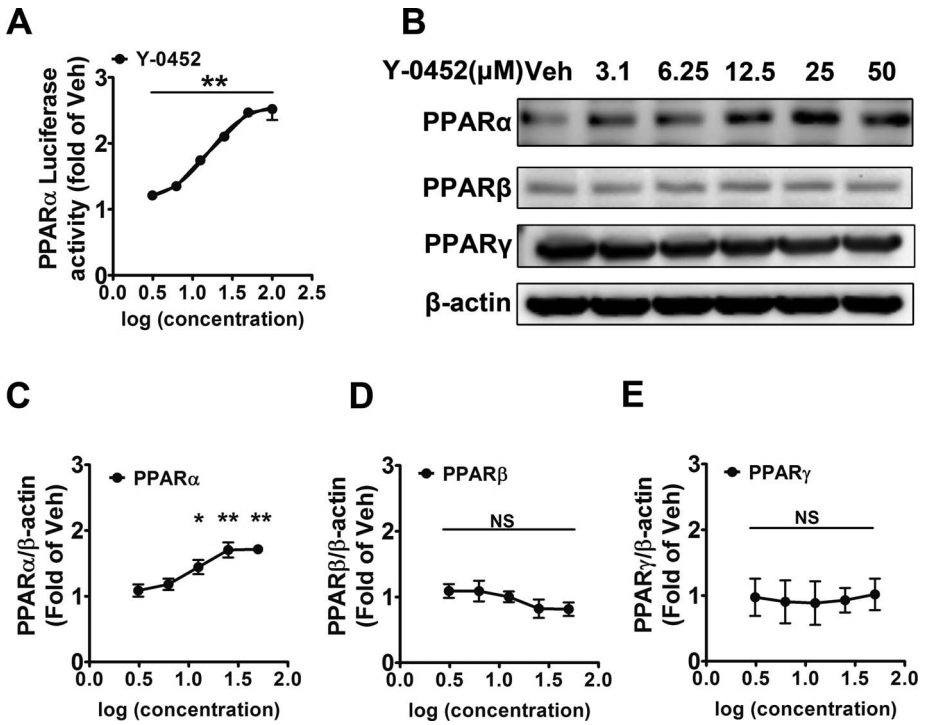

Figure 2. Activation of PPARα and upregulation of PPARα expression by Y-0452. (**A**) Induction of luciferase reporter under the control of PPRE by Y-0452. The PPARα reporter Combo cells were treated with Y-0452 at various concentrations (3.12, 6.25, 12.5, 25, 50, and 100 μM) for 36 hours, and then luciferase activities were measured ($n = 3$, $^{**}P < 0.01$ versus vehicle). (**B**) R28 cells were treated with Y-0452 at indicated concentrations for 24 hours. PPAR protein levels were measured by Western blot analysis with β-actin as loading control. (**C–E**) Densitometry quantification of PPARα, PPARβ, and PPARγ levels ($n = 3$, $^{*}P < 0.05$, $^{**}P < 0.01$, versus vehicle, 1-way ANOVA).

Results

Y-0452 Induced PPARα Transcriptional Activity and Upregulated the Expression of PPARα In Vitro

To evaluate the induction of transcriptional activity of PPARα, we used a commercial PPARα reporter Combo cell line, which stably expresses both PPARα and the luciferase reporter under the control of a promoter containing PPREs. Y-0452 induced the PPRE luciferase activity in a concentration-dependent manner (Fig. 2A), indicating that Y-0452 is a potent agonist for PPARα. In addition, we have compared the activity of Y-0452 with Feno-FA using luciferase assay and showed that Y-0452 has agonist potency similar to that of Feno-FA (Supplementary Fig. S1).

Activation of PPARα is known to upregulate the expression of PPARα.[3,31] To identify if the agonist activity of Y-0452 is specific for PPARα, R28 cells were treated with various concentrations of Y-0452 for 24 hours, and the expression of PPARs was detected by Western blotting. Y-0452 increased protein levels of PPARα in a concentration-dependent manner and did not increase the PPARβ and PPARγ levels under the same conditions, suggesting that it is a specific agonist for PPARα (Figs. 2B–E).

Y-0452 Attenuated Oxidative Stress–Induced Retinal Cell Apoptosis

It is well known that oxidative stress–induced cell apoptosis, especially in retinal neurons, is a pathogenic feature of DR.[32–34] High levels of plasma free fatty acid (FFA) are a common feature of both type 1 and type 2 diabetes.[35] Palmitate, a saturated fatty acid, which makes up 30% to 40% of plasma FFAs, has been implicated in dysfunctions and apoptosis in multiple cell types via activation of NAD(P)H oxidase and NF-κB.[36] Thus, palmitate is commonly used as a diabetic stressor due to its oxidant activity. To evaluate the effect of Y-0452 on the oxidative stress–induced cell death, we performed TUNEL assay in R28 cells exposed to palmitate and different concentrations of Y-0452, or Feno-FA as positive control. Treatment with Y-0452 decreased TUNEL-positive cells in a concentration-dependent manner, similar to Feno-FA (Fig. 3).

Y-0452 Inhibited the NF-κB Pathway

NF-κB, a nuclear transcription factor, regulates the transcription of multiple proinflammatory factors and plays an important role in the pathophysiology of DR.[37,38] Our previous study showed that PPARα alleviated oxidative stress via suppression of the NF-κB pathway.[15] To evaluate the effect of Y-0452 on NF-κB signaling, we examined the expression levels of PPARα, NF-κB, and IκBα in R28 cells. Consistent with previous results, palmitate significantly upregulated phosphorylated NF-κB levels and downregulated IκBα and PPARα levels. Furthermore, Y-0452, similar to Feno-FA, reduced phosphorylated NF-κB levels, while upregulating IκBα and PPARα levels, suggesting that activation of PPARα by Y-0452 can inhibit the NF-κB pathway (Figs. 4A–E).

Y-0452 Inhibited HRCEC Tube Formation and Migration

Retinal vascular endothelial cell migration is an initial and essential process of retinal neovascularization, which is a severe complication of DR.[39] To determine the effect of Y-0452 on endothelial cell migration, scratch wound-healing assay and tube formation assay were performed using primary HRCECs. Compared with the vehicle group, Y-0452–treated HRCECs

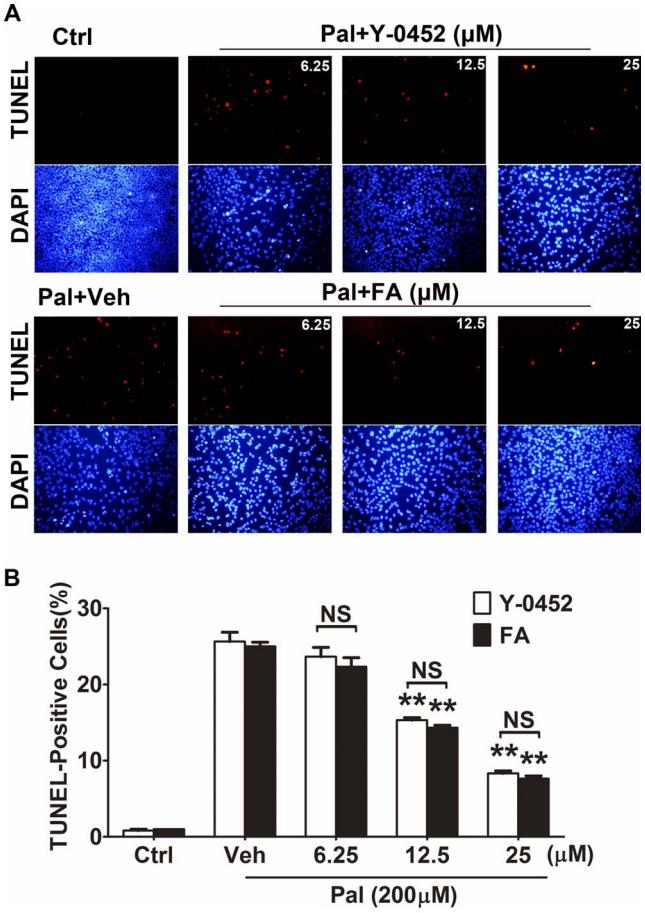

Figure 3. The protective effect of Y-0452 on oxidative stress–induced apoptosis in retinal precursor cells (R28). R28 cells were treated with Y-0452 and Feno-FA (FA) at various concentrations for 4 hours, and 200 μmol/L palmitate (Pal) was added and incubated with the cells for another 24 hours. (**A**) Representative images of TUNEL-positive cells (*red*) and total cells (*blue*, DAPI staining). (**B**) Quantification of TUNEL-positive cells, presented as percentages of total cells ($n = 3$, $^{**}P < 0.01$, 2-way ANOVA).

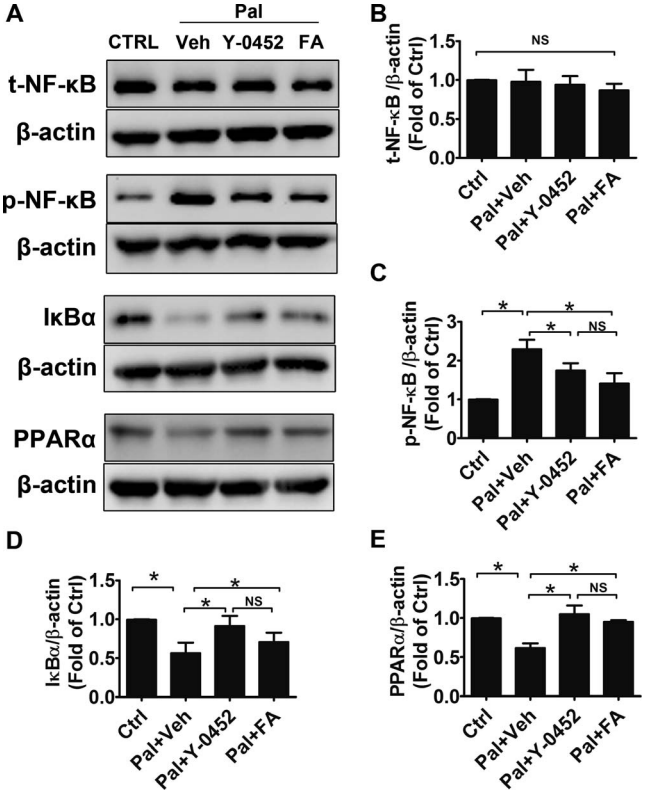

Figure 4. Regulation of inflammation factors by Y-0452. R28 cells were treated with 25 μmol/L Y-0452 for 4 hours and then co-incubated with 200 μmol/L palmitate (Pal) for another 24 hours. (**A**) Levels of total NF-κB (t-NF-κB), phosphorylated NF-κB (p-NF-κB), IκBα, and PPARα were determined by Western blotting. β-actin was used as an internal control. Representative blots were shown from three independent experiments. (**B–E**) Densitometry quantification of t-NF-κB, p-NF-κB, IκBα, and PPARα levels ($n = 3$, $^{*}P<0.05$ versus vehicle, 2-way ANOVA).

showed a significantly decreased tube formation (Figs. 5A, 5C) and migration (Figs. 5B, 5D), with a higher potency than Feno-FA, suggesting that Y-0452 has an antiangiogenic effect.

Effect of Y-0452 on Retinal Vascular Leukostasis and Vascular Leakage in Type 1 Diabetic Rats

Increased leukocytes adherent to vascular endothelium or leukostasis are known to contribute to endothelium impairment and vascular leakage in DR.[40,41] To determine the effects of Y-0452 on leukocyte adherence and vascular leakage in the diabetic retina, rats with STZ-induced diabetes for 1 month received daily intraperitoneal injections of Y-0452 (10 mg/kg/d) or the same volume of vehicle for 3 weeks. Leukostasis assay showed that Y-0452 significantly decreased the adherent leukocytes in the retinal vasculature of diabetic rats (Figs. 6A–D). As shown in Figure 6E, vascular permeability was significantly increased in the diabetic retina, compared with nondiabetic controls. Y-0452 treatment significantly reduced retinal vascular permeability in diabetic rats (Fig. 6E).

In addition, we also measured retinal vascular permeability in rats with 2 months of diabetes treated with Y-0452 for 3 weeks, as well as in OIR rats treated with Y-0452 from the age of P12 to P16. Our results showed that Y-0452 also significantly reduced the vascular permeability in diabetic retinas and OIR retinas (Supplementary Fig. S2). However, retinal thickness in diabetic rats with 2 months of diabetes was not significantly changed after Y-0452 treatment for 3 weeks, compared with vehicle-treated animals (Supplementary Fig. S3). There were no differences in blood glucose and body weight between Y-0452–treated and vehicle-treated groups (Supplementary Table S1).

Effect of Y-0452 on Retinal Function and Retinal Apoptosis in STZ-induced Diabetic Rats

To evaluate the effect of Y-0452 on retinal function and retinal apoptosis in DR models, we measured the photopic and scotopic ERG amplitudes in STZ-induced diabetic rats and quantified the retinal apoptosis using cell death ELISA. Our results showed that both A and B waves of scotopic ERG and the B wave of photopic ERG declined in diabetic rats. Y-0452 treatment showed a rescuing effect on A and B waves of scotopic ERG and the B wave of photopic ERG, suggesting a protective effect on retinal function in DR (Figs. 7A–D). Furthermore, Y-0452 attenuated the increase of retinal DNA fragmentation in diabetic rats, suggesting that Y-0452 ameliorates diabetes-induced retinal apoptosis (Fig. 7E).

In addition, to explore the effect of Y-0452 on retinal pericytes, retinal trypsin digestion was performed in rats with 3 months of diabetes. Our results showed that pericyte

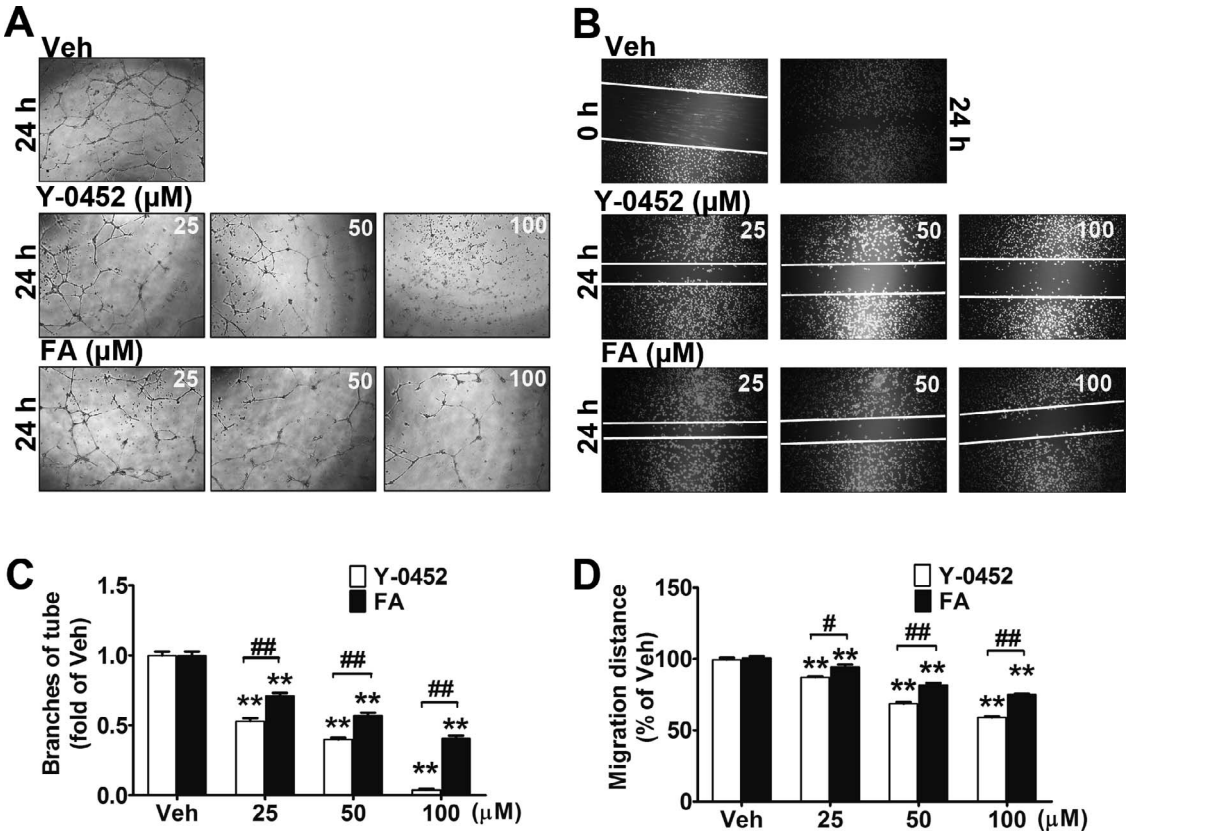

Figure 5. Inhibitory effects of Y-0452 on endothelial cell migration and tube formation. (**A**, **C**) HRCECs were treated with Y-0452 and Feno-FA (FA) at indicated concentrations for 16 hours and seeded onto Matrigel containing different concentrations of Y-0452 or Feno-FA. After 6 hours of incubation, branch numbers were counted in five random fields under a microscope. (**B**, **D**) HRCECs were seeded in a 24-well plate and cultured in growth medium until 80% confluency. A straight line across the center of the well was scratched. After washing with PBS, cells were incubated with different concentrations of Y-0452 and Feno-FA for 24 hours. Images were captured, and cell migration distances were quantified using ImageJ software and expressed as percentages of vehicle control ($n = 3$, $^{**}P < 0.01$ versus vehicle, $^{\#}P < 0.05$ versus Feno-FA, $^{\#\#}P < 0.01$ versus Feno-FA, 2-way ANOVA).

numbers in diabetic retinas were significantly decreased, compared with nondiabetic retinas, and the decrease was attenuated in Y-0452–treated animals, compared with that in vehicle-treated controls (Supplementary Fig. S4).

Effect of Y-0452 on Retinal Apoptosis and Inflammation in OIR Model

To further evaluate the effect of Y-0452 on retinal apoptosis and inflammation in ischemia-induced retinopathy, WT OIR mice received daily intraperitoneal injections of Y-0452 (10 mg/kg/d) or the same volume of the vehicle from age of P12 to P16. Our results showed that TUNEL-positive cells were increased in OIR retinas, and most TUNEL-positive cells were not costained with CD31, an endothelial cell marker. TUNEL-positive cells were significantly decreased by Y-0452 treatment (Figs. 8A, 8C). Furthermore, the adherent leukocytes in OIR retinal vessels were also decreased by Y-0452 (Figs. 8B, 8D).

Effect of Y-0452 on the Retinal Neovascularization in OIR Mice

Retinal neovascularization is a common feature of most ischemic retinopathies, and OIR is a commonly used model to study retinal neovascularization.[42] To evaluate the function of Y-0452 on retinal neovascularization, WT and *PPARα*$^{-/-}$ OIR mice were intraperitoneally injected with Y-0452 (10 mg/kg/d) from P12 to P16 or the same volume of vehicle. As shown by vessel staining in flat-mounted retina, areas of retinal neovascularization and vaso-obliteration were significantly reduced in the WT OIR mice treated with Y-0452, compared with the vehicle group. In *PPARα*$^{-/-}$ OIR mice, however, Y-0452 treatment did not decrease retinal neovascularization and avascular areas (Figs. 9A–C), suggesting that the antiangiogenic effect of Y-0452 is PPARα-dependent. Accordingly, Y-0452 significantly reduced retinal VEGF and TNF-α levels in WT OIR mice, but not in *PPARα*$^{-/-}$ OIR mice (Figs. 9D–F).

No Changes in Liver and Kidney Histologic Structures After Y-0452 Treatment

To evaluate possible systemic adverse effects of Y-0452, we examined the histologic structures of the liver and kidney in rats. BN rats at the age of 2 months received daily intraperitoneal injections of Y-0452 (10 mg/kg/d) or the same volume of the vehicle for 3 weeks ($n = 6$). Hematoxylin-eosin staining of liver and kidney sections was performed after the treatment. There were no significant changes in liver and kidney histologic structures between Y-0452 treated and vehicle control groups (Supplementary Fig. S5).

Discussion

PPARα is a ligand-activated transcription factor and is highly expressed in oxidative tissues, such as the liver, kidney, heart,

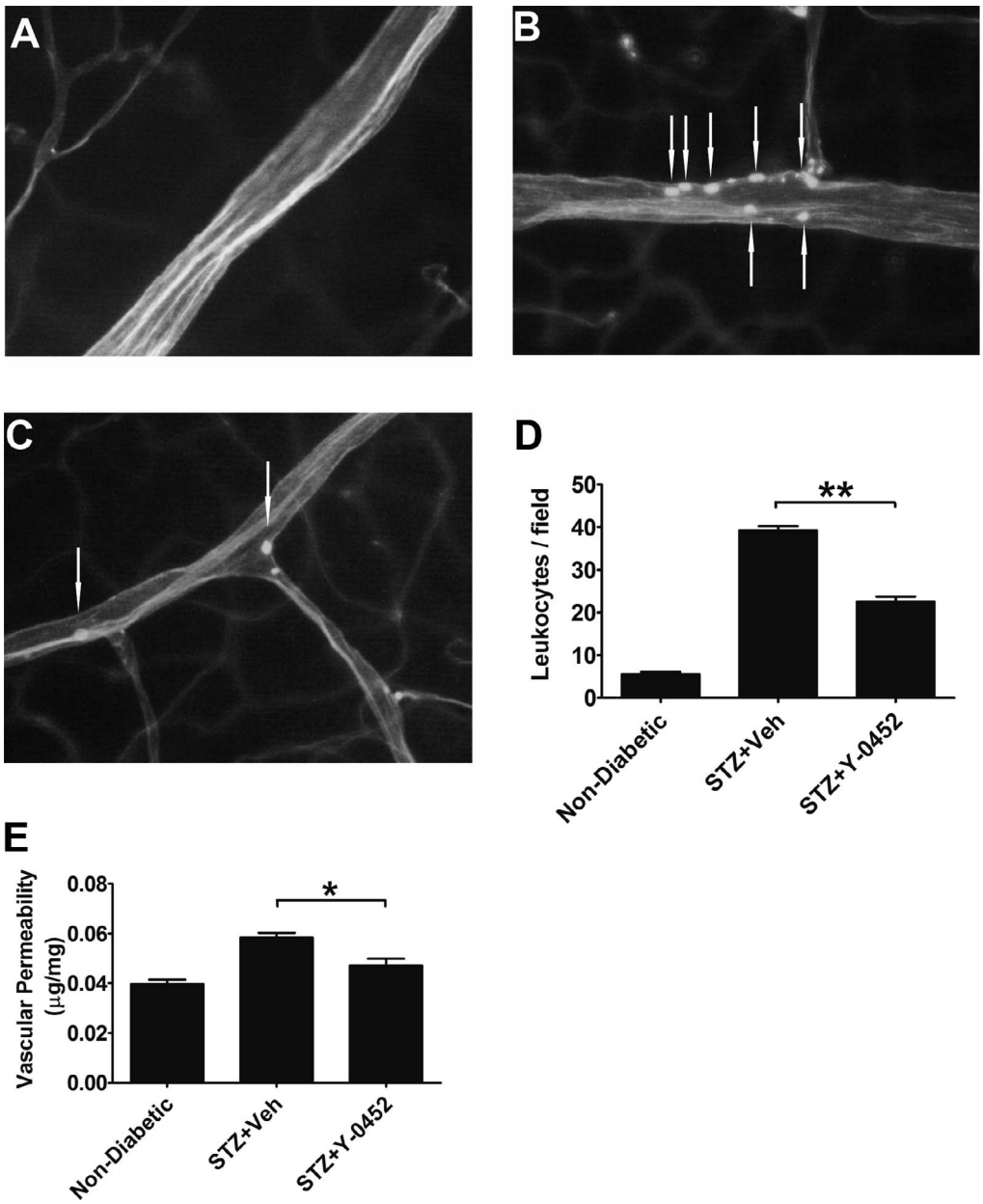

Figure 6. Effects of Y-0452 on retinal vascular inflammation and leakage in diabetic rats. Rats with 1 month of STZ-induced diabetes received daily intraperitoneal injections of Y-0452 (10 mg/kg/d) or the same volume of the vehicle (Veh) as a control for 3 weeks. Retinal vascular endothelial cells and adherent leukocytes were stained with FITC–concanavalin-A and visualized under a fluorescence microscope. (**A–C**) Representative images of retinal adherent leukocytes in nondiabetic and STZ-induced diabetic rats ([**A**] nondiabetic, [**B**] STZ+Veh, [**C**] STZ+Y-0452). (**D**) Quantification of retinal adherent leukocytes was performed from ×40 magnification images. Adherent leukocytes were counted in six random fields per retina (*white arrows* indicate adherent leukocytes). (**E**) Retinal vascular leakage was measured using Evans blue as a tracer and normalized by total retinal protein concentrations ($n = 6$; $^{*}P < 0.05$, $^{**}P < 0.01$, 2-way ANOVA).

and adipose tissue.[43,44] PPARα plays a vital role in the regulation of lipid metabolism and has been used as a therapeutic target for hyperlipidemia.[45–47] Two prospective clinical trials (FIELD and ACCORD) have reported that the PPARα agonist fenofibrate has a robust and unanticipated therapeutic effect on DR.[10,11] Our previous studies have shown that decreased PPARα expression in diabetic retinas contributes to retinal inflammation and neovascularization in DR, and activation of PPARα has anti-inflammatory and antiapoptotic effects in OIR and diabetic animal models through suppression of NF-κB signaling.[3,15,48] These findings prompted us to search for novel PPARα agonists with different chemical structures than fenofibrate for the treatment of DR. In the present study, we identified a novel PPARα agonist, a phenylquinoline derivative with a completely different structure than existing PPARα agonists. This novel agonist also activated PPARα and displayed anti-inflammatory, antiangiogenic, and neuroprotective effects in the retinas of DR animal models, suggesting therapeutic potential for the treatment of DR.

Retinal cell apoptosis plays an important role in the pathogenesis of DR. Apoptosis in retinal vascular endothelial cells, pericytes, and retinal neuronal cells has been shown to result in impaired retinal microvascular structure, vascular

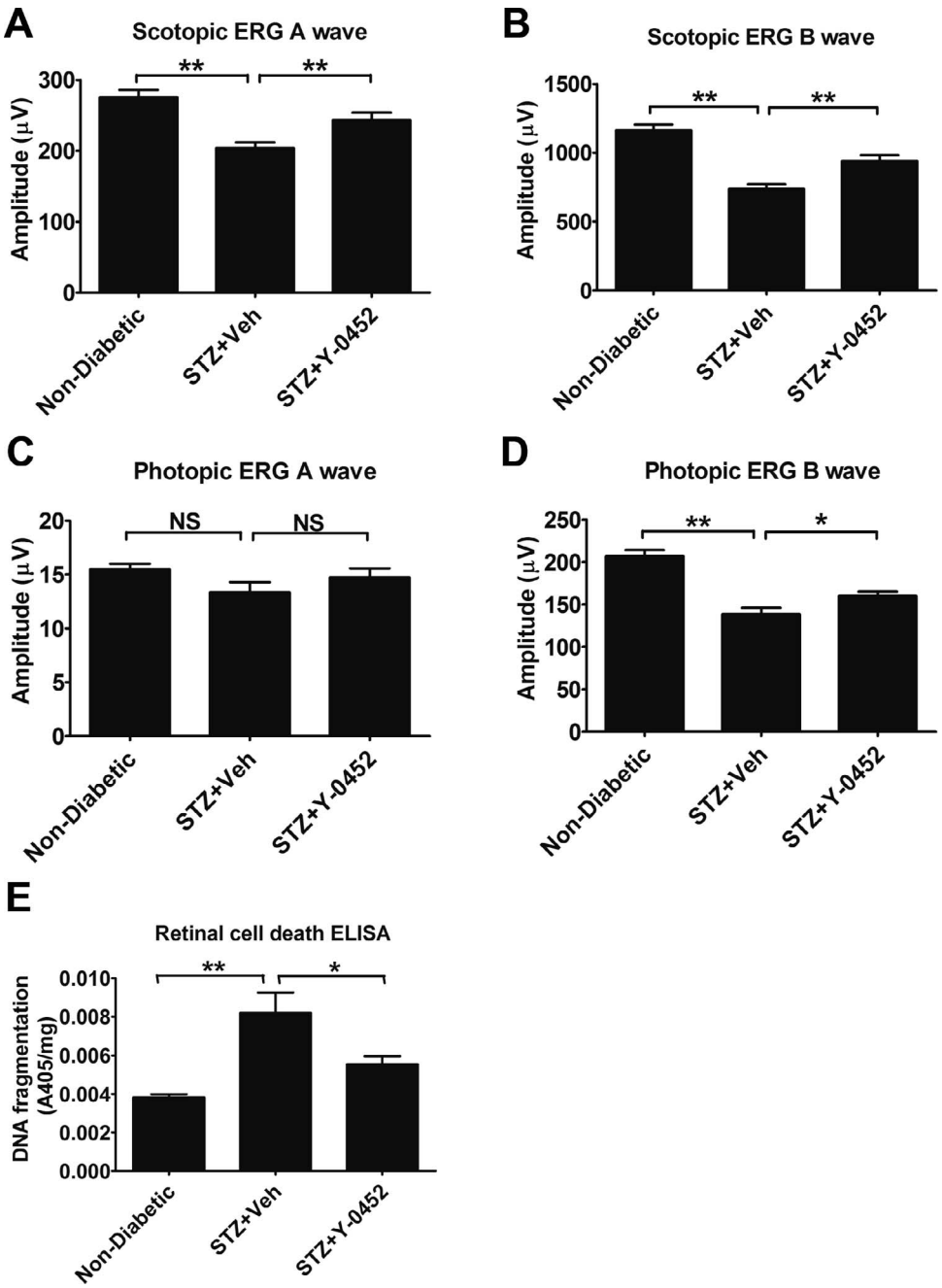

Figure 7. Effects of Y-0452 on ERG responses and retinal cell death in STZ-induced diabetic rats. Rats with 2 months of diabetes and treated with Y-0452 for 3 weeks were used for ERG recording and retinal DNA fragmentation ELISA. (**A–D**) Scotopic and photopic ERG A and B wave amplitudes in the indicated groups ($n = 6$; $^{*}P < 0.05$, $^{**}P < 0.01$). (**E**) Quantification of retinal DNA fragmentation, reflective of total retinal apoptosis, in the retina of nondiabetic and STZ-induced diabetic rats treated with Y-0452 and vehicle ($n = 6$; $^{*}P < 0.05$, $^{**}P < 0.01$, 2-way ANOVA).

leakage, macular edema, and eventually vision loss.[49–52] In our recent study, we have shown that PPARα has protective effects against pericyte loss in a diabetic animal model via suppressing NF-κB signaling.[15] To determine the protective effects of Y-0452 on retinal neurons, we used R28 cells, a commonly used cell line from retinal precursor cells.[24,53] Our results showed that Y-0452 reduced the oxidative stress–induced apoptosis of the retinal precursor cells in vitro. In diabetic rats, administration of Y-0452 alleviated the retinal apoptosis and attenuated the activation of NF-κB, suggesting that activation of PPARα by Y-0452 has a potent neuroprotective effect on retinal neuronal cells under diabetic conditions. Further, to identify the retinal cell types involved in the antiapoptotic effect of Y-0452, we performed TUNEL assay in retina cross sections with costaining of an endothelial cell marker CD31. Our results demonstrated that most TUNEL-positive cells are not colocalized with CD31, suggesting that the protective effect of Y-0452 against apoptosis occurs in either retinal neurons or glial cells. The retina-protective effect of Y-0452 was also supported by the retinal function assay, as Y-0452 prevented the decline of scotopic and photopic ERG of diabetic rats.

It has been reported that some inflammatory factors, such as VEGF, MCP-1, TNF-α, and ICAM-1, are upregulated in the retina of diabetic animal models and patients with DR, leading

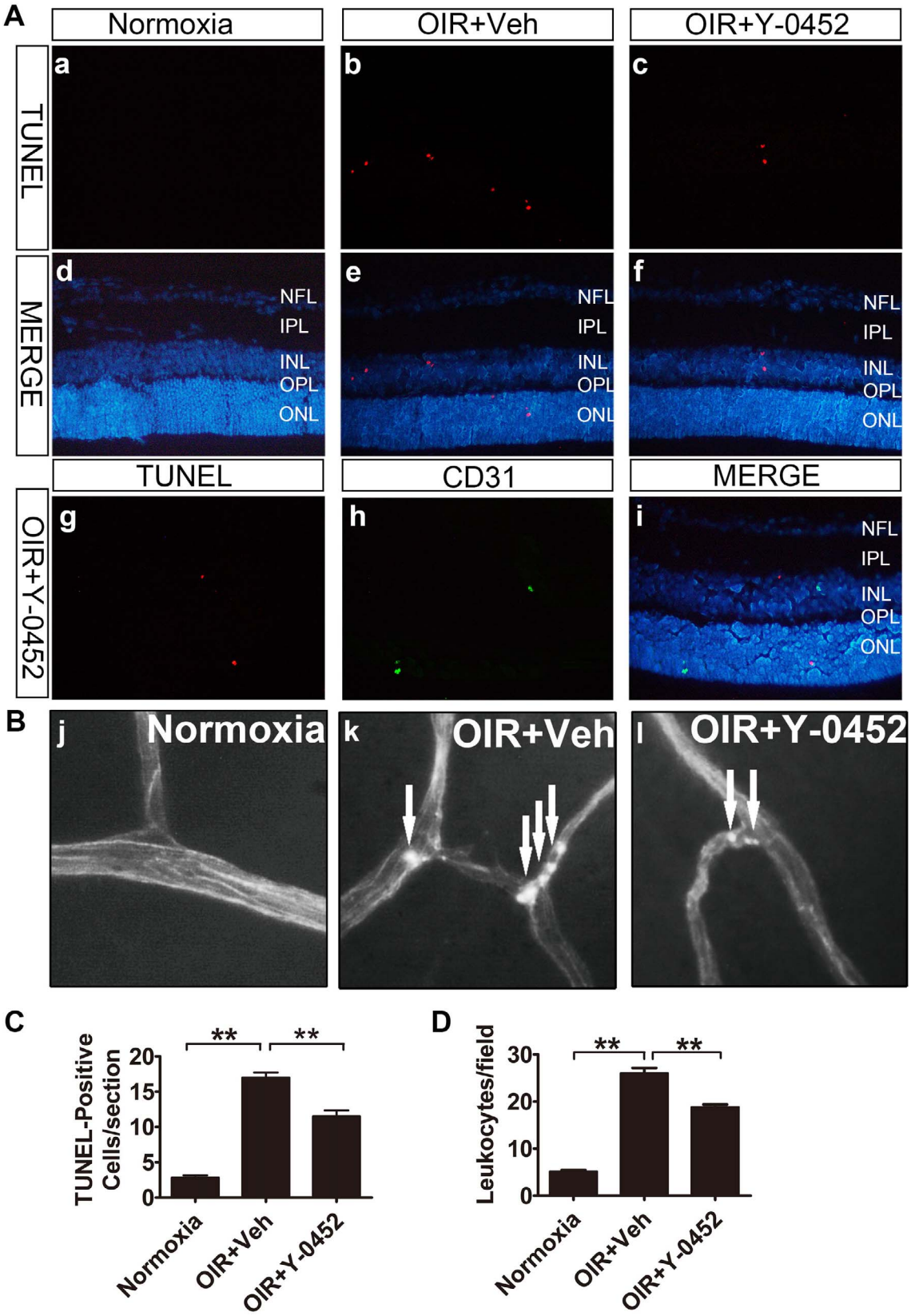

Figure 8. Effects of Y-0452 on retinal apoptosis and inflammation in OIR mice. WT OIR mice were intraperitoneally injected with Y-0452 (10 mg/kg/d) from P12 to P16 or the same volume of vehicle. (**A**) Representative images of retinal apoptotic cells in OIR mice (normoxia: [**a**, **d**], OIR+Veh: [**b**, **e**], OIR+Y-0452: [**c**, **f**], costaining with anti-CD31: [**g–i**]). Retinal apoptotic cells were labeled by TUNEL (*red*), and nuclei stained with DAPI (*blue*). CD31 (*green*) cells were co-immunostained with TUNEL (*red*) and DAPI (*blue*) in OIR retinal sections. (**B**) Representative images of retinal adherent leukocytes in OIR mice (*white arrows* indicate adherent leukocytes). (**C**) Quantification of retinal TUNEL-positive cells in OIR mice from retinal sections ($n = 6$; $^{*}P < 0.05$, $^{**}P < 0.01$ versus vehicle, 1-way ANOVA). (**D**) Quantification of retinal adherent leukocytes in OIR mice was performed from ×40 magnification images. Adherent leukocytes were counted in six random fields per retina ($n = 6$; $^{*}P < 0.05$, $^{**}P < 0.01$ versus vehicle, 2-way ANOVA).

Investigative Ophthalmology & Visual Science

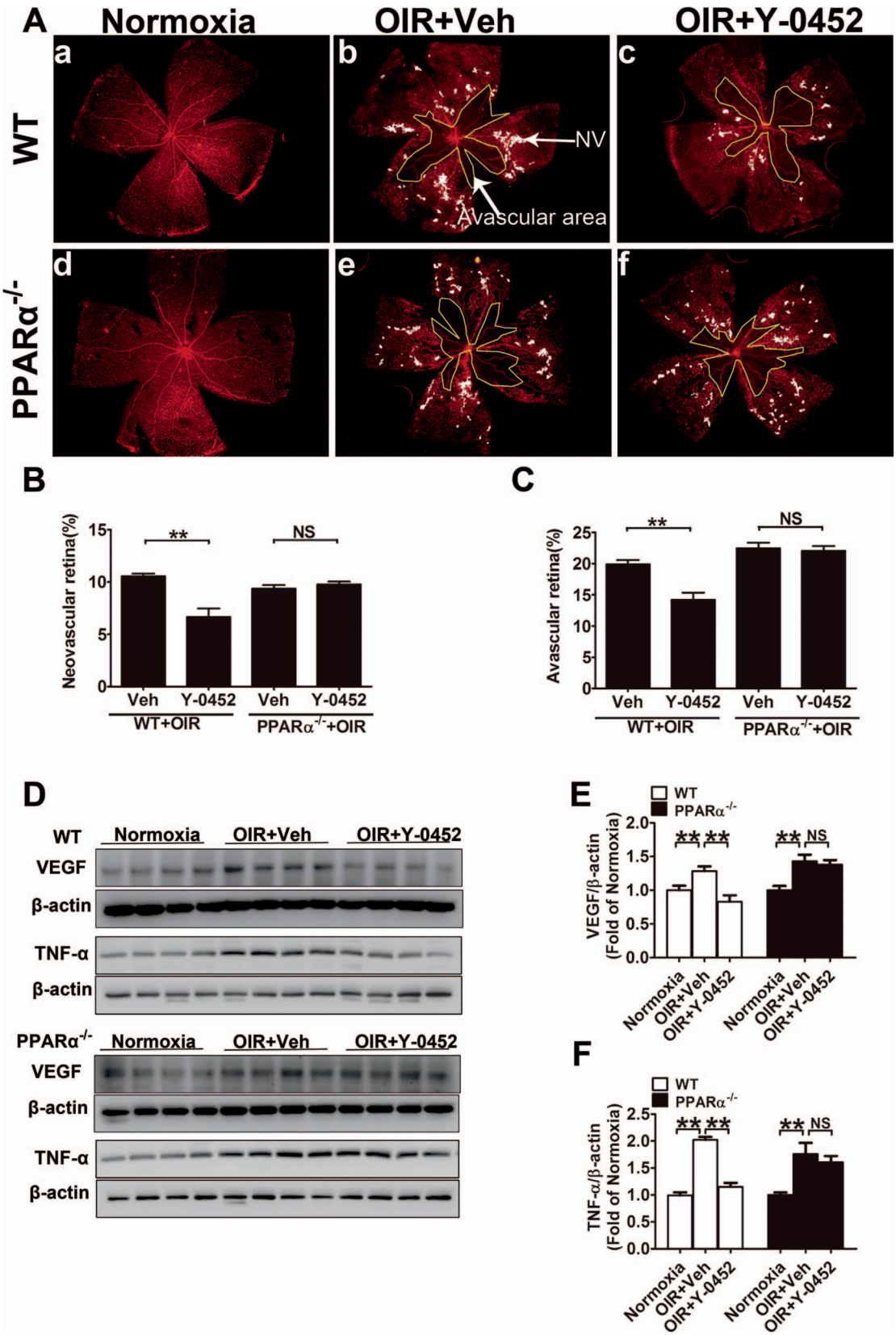

Figure 9. Effect of Y-0452 on retinal neovascularization in OIR mice. WT and *PPARα*$^{-/-}$ OIR mice were intraperitoneally injected with Y-0452 (10 mg/kg/d) from P12 to P16 or the same volume of vehicle. The retinas were fixed and stained with Isolectin B4. Areas of retinal neovascularization and vaso-obliteration were quantified under a fluorescence microscope. (**A**) Representative images of retinal neovascularization and avascular areas in WT (**a–c**) and *PPARα*$^{-/-}$ OIR mice (**d–f**). The *white dot–marked area* indicates neovascular retina and the *yellow line–marked area* indicates avascular area. (**B**, **C**) Quantification of retinal neovascularization and avascular areas. (**D**) Retinal VEGF and TNF-α levels were measured by Western blot analysis. (**E**, **F**) Quantification of VEGF levels in WT and *PPARα*$^{-/-}$ OIR mice ($n = 8$; $^{*}P < 0.05$, $^{**}P < 0.01$, 2-way ANOVA).

Investigative Ophthalmology & Visual Science

to the impairment of vascular endothelium and vascular leakage.[54–60] The increased inflammatory factors contribute to leukocyte adhesion and apoptosis of endothelial cells and pericytes, which may result in the breakdown of the blood-retinal barrier.[61–65] We recently demonstrated that PPARα exerts a potent anti-inflammatory effect under diabetic conditions through suppression of the expression of ICAM-1, TNF-α, and VEGF, suggesting that PPARα could be a promising therapeutic target for retinal inflammation in DR. To identify the effect on inflammation of the novel PPARα agonist in diabetic models, adherent leukocytes in retinal vasculature, retinal vascular permeability, and expression of inflammatory cytokines were measured in diabetic rats and OIR mice. The results demonstrated that Y-0452 attenuated the increases of retinal vascular leakage and reduced the adherent leukocytes in diabetic and OIR models. Also, Y-0452 alleviates the overexpression of inflammatory factors in OIR retinas, such as VEGF and TNF-α. These findings suggest that Y-0452 is a potential drug candidate for the treatment of DR, especially for retinal inflammation in early stages of DR; however, the retinal thickness did not change in diabetic rats treated with this compound compared with vehicle control. One of the reasons might be the treatment period of 3 weeks is not long enough to result in any significant change of retinal thickness. Retinal neovascularization is a common feature leading to vision loss in DR.[66] VEGF plays a crucial role in the process of the pathologic retinal angiogenesis by promoting the proliferation and migration of retinal capillary endothelial cells in proliferative DR.[67,68] In our previous study, we demonstrated that overexpression of PPARα significantly inhibits the endothelial cell migration and tube formation.[48] Moreover, intravitreal injection of fenofibrate downregulates VEGF expression in the retinas of OIR animals.[48] In the present study, Y-0452 also showed an inhibitory effect on endothelial cell migration and tube formation in a concentration-dependent manner. Also, Y-0452 administration reduced retinal neovascularization and vaso-obliteration in WT OIR mice. To determine if the antiangiogenic effect of Y-0452 is indeed through PPARα activation, we also used *PPARα*$^{-/-}$ mice with OIR, and found that PPARα ablation abolished antiangiogenic effects of Y-0452. Furthermore, the VEGF and TNF-α expression is downregulated by Y-0452 in WT OIR retinas, and the inhibitory effect on VEGF and TNF-α is abolished in *PPARα*$^{-/-}$ OIR mice. These observations indicate that Y-0452 exerts antiangiogenic effects in OIR retinas through a PPARα-dependent mechanism.

The present study identified a novel PPARα agonist that reduces retinal inflammation and apoptosis in a diabetic model, as well as retinal neovascularization in the OIR model. Furthermore, Y-0452 exerts its effects through activation of PPARα, leading to suppression of activation of NF-κB signaling under diabetes conditions. In addition, Y-0452 had no significant toxic effects, as shown by analysis of body weight, blood glucose, and kidney and liver histological structures. These findings suggest that Y-0452 is a promising drug candidate for the treatment of DR.

Acknowledgments

The authors thank the Diabetic Animal Core and Histology and Imaging Core in the diabetes Center of Biological Research Excellence for technical assistance.

Supported by National Institutes of Health grants EY012231, EY018659, EY019309, GM104934, and GM122744; a grant from Juvenile Diabetes Research Foundation; and Oklahoma Center for the Advancement of Science & Technology grant HR16-041.

Disclosure: **G. Deng**, None; **E.P. Moran**, None; **R. Cheng**, None; **G. Matlock**, None; **K. Zhou**, None; **D. Moran**, None; **D. Chen**, None; **Q. Yu**, None; **J.-X. Ma**, None

References

1. Fong DS, Sharza M, Chen W, Paschal JF, Ariyasu RG, Lee PP. Vision loss among diabetics in a group model Health Maintenance Organization (HMO). *Am J Ophthalmol*. 2002; 133:236–241.
2. Deliyanti D, Zhang Y, Khong F, et al. FT011, a novel cardiorenal protective drug, reduces inflammation, gliosis and vascular injury in rats with diabetic retinopathy. *PLoS One*. 2015;10:e0134392.
3. Hu Y, Chen Y, Ding L, et al. Pathogenic role of diabetes-induced PPAR-alpha down-regulation in microvascular dysfunction. *Proc Natl Acad Sci U S A*. 2013;110:15401–15406.
4. Xie TY, Yan W, Lou J, Chen XY. Effect of ozone on vascular endothelial growth factor (VEGF) and related inflammatory cytokines in rats with diabetic retinopathy. *Genet Mol Res*. 2016;15:1–11.
5. Gao X, Li Y, Wang H, Li C, Ding J. Inhibition of HIF-1alpha decreases expression of pro-inflammatory IL-6 and TNF-alpha in diabetic retinopathy [published online ahead of print June 11, 2016]. *Acta Ophthalmol*. doi:10.1111/aos.13096.
6. Kadlubowska J, Malaguarnera L, Waz P, Zorena K. Neurodegeneration and neuroinflammation in diabetic retinopathy: potential approaches to delay neuronal loss. *Curr Neuropharmacol*. 2016;14:831–839.
7. Barber AJ, Lieth E, Khin SA, Antonetti DA, Buchanan AG, Gardner TW. Neural apoptosis in the retina during experimental and human diabetes. Early onset and effect of insulin. *J Clin Invest*. 1998;102:783–791.
8. Lieth E, Gardner TW, Barber AJ, Antonetti DA; for the Penn State Retina Research Group. Retinal neurodegeneration: early pathology in diabetes. *Clin Exp Ophthalmol*. 2000;28:3–8.
9. Mizutani M, Gerhardinger C, Lorenzi M. Muller cell changes in human diabetic retinopathy. *Diabetes*. 1998;47:445–449.
10. Keech AC, Mitchell P, Summanen PA, et al. Effect of fenofibrate on the need for laser treatment for diabetic retinopathy (FIELD study): a randomised controlled trial. *Lancet*. 2007;370:1687–1697.
11. Group AS, Group AES, Chew EY, et al. Effects of medical therapies on retinopathy progression in type 2 diabetes. *N Engl J Med*. 2010;363:233–244.
12. Capozzi ME, McCollum GW, Savage SR, Penn JS. Peroxisome proliferator-activated receptor-beta/delta regulates angiogenic cell behaviors and oxygen-induced retinopathy. *Invest Ophthalmol Vis Sci*. 2013;54:4197–4207.
13. Tawfik A, Sanders T, Kahook K, Akeel S, Elmarakby A, Al-Shabrawey M. Suppression of retinal peroxisome proliferator-activated receptor gamma in experimental diabetes and oxygen-induced retinopathy: role of NADPH oxidase. *Invest Ophthalmol Vis Sci*. 2009;50:878–884.
14. Zhao S, Li J, Wang N, et al. Feno fibrate suppresses cellular metabolic memory of high glucose in diabetic retinopathy via a sirtuin 1-dependent signalling pathway. *Mol Med Rep*. 2015; 12:6112–6118.
15. Ding L, Cheng R, Hu Y, et al. Peroxisome proliferator-activated receptor alpha protects capillary pericytes in the retina. *Am J Pathol*. 2014;184:2709–2720.
16. Deplanque D, Gele P, Petrault O, et al. Peroxisome proliferator-activated receptor-alpha activation as a mechanism of preventive neuroprotection induced by chronic fenofibrate treatment. *J Neurosci*. 2003;23:6264–6271.
17. Cho YR, Lim JH, Kim MY, et al. Therapeutic effects of fenofibrate on diabetic peripheral neuropathy by improving endothelial and neural survival in db/db mice. *PLoS One*. 2014;9:e83204.
18. Brown WR, Thore CR. Review: cerebral microvascular pathology in ageing and neurodegeneration. *Neuropathol Appl Neurobiol*. 2011;37:56–74.

19. Antonetti DA, Klein R, Gardner TW. Diabetic retinopathy. *N Engl J Med*. 2012;366:1227–1239.
20. Bordet R, Ouk T, Petrault O, et al. PPAR: a new pharmacological target for neuroprotection in stroke and neurodegenerative diseases. *Biochem Soc Trans*. 2006;34:1341–1346.
21. Hiukka A, Maranghi M, Matikainen N, Taskinen MR. PPARalpha: an emerging therapeutic target in diabetic microvascular damage. *Nat Rev Endocrinol*. 2010;6:454–463.
22. Mysiorek C, Culot M, Dehouck L, et al. Peroxisome-proliferator-activated receptor-alpha activation protects brain capillary endothelial cells from oxygen-glucose deprivation-induced hyperpermeability in the blood-brain barrier. *Curr Neurovasc Res*. 2009;6:181–193.
23. Lefebvre P, Chinetti G, Fruchart JC, Staels B. Sorting out the roles of PPAR alpha in energy metabolism and vascular homeostasis. *J Clin Invest*. 2006;116:571–580.
24. Seigel GM. Review: R28 retinal precursor cells: the first 20 years. *Mol Vis*. 2014;20:301–306.
25. Smith LE, Wesolowski E, McLellan A, et al. Oxygen-induced retinopathy in the mouse. *Invest Ophthalmol Vis Sci*. 1994; 35:101–111.
26. Abcouwer SF, Lin CM, Wolpert EB, et al. Effects of ischemic preconditioning and bevacizumab on apoptosis and vascular permeability following retinal ischemia-reperfusion injury. *Invest Ophthalmol Vis Sci*. 2010;51:5920–5933.
27. Xu Q, Qaum T, Adamis AP. Sensitive blood-retinal barrier breakdown quantitation using Evans blue. *Invest Ophthalmol Vis Sci*. 2001;42:789–794.
28. Ishida S, Usui T, Yamashiro K, et al. VEGF164 is proinflammatory in the diabetic retina. *Invest Ophthalmol Vis Sci*. 2003; 44:2155–2162.
29. Moran E, Ding L, Wang Z, et al. Protective and antioxidant effects of PPARalpha in the ischemic retina. *Invest Ophthalmol Vis Sci*. 2014;55:4568–4576.
30. Connor KM, Krah NM, Dennison RJ, et al. Quantification of oxygen-induced retinopathy in the mouse: a model of vessel loss, vessel regrowth and pathological angiogenesis. *Nat Protoc*. 2009;4:1565–1573.
31. Velkov T, Rimmer KA, Headey SJ. Ligand-enhanced expression and in-cell assay of human peroxisome proliferator-activated receptor alpha ligand binding domain. *Protein Expr Purif*. 2010;70:260–269.
32. Al-Shabrawey M, Smith S. Prediction of diabetic retinopathy: role of oxidative stress and relevance of apoptotic biomarkers. *EPMA J*. 2010;1:56–72.
33. Feenstra DJ, Yego EC, Mohr S. Modes of retinal cell death in diabetic retinopathy. *J Clin Exp Ophthalmol*. 2013;4:298.
34. Kowluru RA, Chan PS. Oxidative stress and diabetic retinopathy. *Exp Diabetes Res*. 2007;2007:43603.
35. Pankow JS, Duncan BB, Schmidt MI, et al. Fasting plasma free fatty acids and risk of type 2 diabetes: the atherosclerosis risk in communities study. *Diabetes Care*. 2004;27:77–82.
36. Cacicedo JM, Benjachareowong S, Chou E, Ruderman NB, Ido Y. Palmitate-induced apoptosis in cultured bovine retinal pericytes: roles of NAD(P)H oxidase, oxidant stress, and ceramide. *Diabetes*. 2005;54:1838–1845.
37. Tang J, Kern TS. Inflammation in diabetic retinopathy. *Prog Retin Eye Res*. 2011;30:343–358.
38. Patel S, Santani D. Role of NF-kappa B in the pathogenesis of diabetes and its associated complications. *Pharmacol Rep*. 2009;61:595–603.
39. Bharadwaj AS, Appukuttan B, Wilmarth PA, et al. Role of the retinal vascular endothelial cell in ocular disease. *Prog Retin Eye Res*. 2013;32:102–180.
40. Semeraro F, Cancarini A, dell'Omo R, Rezzola S, Romano MR, Costagliola C. Diabetic retinopathy: vascular and inflammatory disease. *J Diabetes Res*. 2015;2015:582060.
41. Tarr JM, Kaul K, Chopra M, Kohner EM, Chibber R. Pathophysiology of diabetic retinopathy. *ISRN Ophthalmol*. 2013;2013:343560.
42. Scott A, Fruttiger M. Oxygen-induced retinopathy: a model for vascular pathology in the retina. *Eye (Lond)*. 2010;24:416–421.
43. Chinetti G, Fruchart JC, Staels B. Peroxisome proliferator-activated receptors (PPARs): nuclear receptors at the crossroads between lipid metabolism and inflammation. *Inflamm Res*. 2000;49:497–505.
44. Mazzatti DJ, Karnik K, Oita RC, Powell JR. Insulin resistance, chronic inflammation and the link with immunosenescence. In: Tamas F, Claudio F, Katsuiku H, Graham P, eds. *Handbook on Immunosenescence*. Dordecht: Springer; 2009:1247–1272.
45. Beaven SW, Tontonoz P. Nuclear receptors in lipid metabolism: targeting the heart of dyslipidemia. *Ann Rev Med*. 2006; 57:313–329.
46. Monsalve FA, Pyarasani RD, Delgado-Lopez F, Moore-Carrasco R. Peroxisome proliferator-activated receptor targets for the treatment of metabolic diseases. *Mediators Inflamm*. 2013; 2013:549627.
47. Staels B, Fruchart JC. Therapeutic roles of peroxisome proliferator-activated receptor agonists. *Diabetes*. 2005;54: 2460–2470.
48. Chen Y, Hu Y, Lin M, et al. Therapeutic effects of PPARalpha agonists on diabetic retinopathy in type 1 diabetes models. *Diabetes*. 2013;62:261–272.
49. Barber AJ. A new view of diabetic retinopathy: a neurodegenerative disease of the eye. *Prog Neuropsychopharmacol Biol Psychiatry*. 2003;27:283–290.
50. Behl Y, Krothapalli P, Desta T, DiPiazza A, Roy S, Graves DT. Diabetes-enhanced tumor necrosis factor-alpha production promotes apoptosis and the loss of retinal microvascular cells in type 1 and type 2 models of diabetic retinopathy. *Am J Pathol*. 2008;172:1411–1418.
51. Geraldes P, Hiraoka-Yamamoto J, Matsumoto M, et al. Activation of PKC-delta and SHP-1 by hyperglycemia causes vascular cell apoptosis and diabetic retinopathy. *Nat Med*. 2009;15:1298–1306.
52. Mizutani M, Kern TS, Lorenzi M. Accelerated death of retinal microvascular cells in human and experimental diabetic retinopathy. *J Clin Invest*. 1996;97:2883–2890.
53. Gardner T, Gong L, He S, Arnold E, Fort P, Abcouwer S. Prevention of caspase activation and apoptotic death of R28 retinal neuronal cells by IGF-1 corresponds with AKT-dependent inhibition of FOXO1 function. *Invest Ophthalmol Vis Sci*. 2013;54:3689–3689.
54. Elner SG, Elner VM, Jaffe GJ, Stuart A, Kunkel SL, Strieter RM. Cytokines in proliferative diabetic retinopathy and proliferative vitreoretinopathy. *Curr Eye Res*. 1995;14:1045–1053.
55. Gardiner TA, Gibson DS, de Gooyer TE, de la Cruz VF, McDonald DM, Stitt AW. Inhibition of tumor necrosis factor-α improves physiological angiogenesis and reduces pathological neovascularization in ischemic retinopathy. *Am J Pathol*. 2005;166:637–644.
56. Meleth AD, Agron E, Chan CC, et al. Serum inflammatory markers in diabetic retinopathy. *Invest Ophthalmol Vis Sci*. 2005;46:4295–4301.
57. Mitamura Y, Takeuchi S, Matsuda A, Tagawa Y, Mizue Y, Nishihira J. Monocyte chemotactic protein-1 in the vitreous of patients with proliferative diabetic retinopathy. *Ophthalmologica*. 2001;215:415–418.
58. Mysliwiec M, Balcerska A, Zorena K, Mysliwska J, Lipowski P, Raczynska K. The assessment of the correlation between vascular endothelial growth factor (VEGF), tumor necrosis factor (TNF-alpha), interleukin 6 (IL-6), glycaemic control (HbA1c) and the development of the diabetic retinopathy in

Investigative Ophthalmology & Visual Science

children with diabetes mellitus type 1 [in Polish]. *Klin Oczna*. 2007;109:150–154.

59. Yoshida S, Yoshida A, Ishibashi T, Elner SG, Elner VM. Role of MCP-1 and MIP-1alpha in retinal neovascularization during postischemic inflammation in a mouse model of retinal neovascularization. *J Leukoc Biol*. 2003;73:137–144.
60. Bartoli M, Al-Shabrawey M, Labazi M, et al. HMG-CoA reductase inhibitors (statin) prevents retinal neovascularization in a model of oxygen-induced retinopathy. *Invest Ophthalmol Vis Sci*. 2009;50:4934–4940.
61. Antonetti DA, Lieth E, Barber AJ, Gardner TW. Molecular mechanisms of vascular permeability in diabetic retinopathy. *Semin Ophthalmol*. 1999;14:240–248.
62. Joussen AM, Poulaki V, Le ML, et al. A central role for inflammation in the pathogenesis of diabetic retinopathy. *FASEB J*. 2004;18:1450–1452.
63. Leal EC, Manivannan A, Hosoya K, et al. Inducible nitric oxide synthase isoform is a key mediator of leukostasis and blood-retinal barrier breakdown in diabetic retinopathy. *Invest Ophthalmol Vis Sci*. 2007;48:5257–5265.
64. Qaum T, Xu Q, Joussen AM, et al. VEGF-initiated blood-retinal barrier breakdown in early diabetes. *Invest Ophthalmol Vis Sci*. 2001;42:2408–2413.
65. Murata T, Nakagawa K, Khalil A, Ishibashi T, Inomata H, Sueishi K. The relation between expression of vascular endothelial growth factor and breakdown of the blood-retinal barrier in diabetic rat retinas. *Lab Invest*. 1996;74:819–825.
66. Milne R, Brownstein S. Advanced glycation end products and diabetic retinopathy. *Amino Acids*. 2013;44:1397–1407.
67. Duh EJ, Yang HS, Suzuma I, et al. Pigment epithelium-derived factor suppresses ischemia-induced retinal neovascularization and VEGF-induced migration and growth. *Invest Ophthalmol Vis Sci*. 2002;43:821–829.
68. Otani A, Takagi H, Suzuma K, Honda Y. Angiotensin II potentiates vascular endothelial growth factor-induced angiogenic activity in retinal microcapillary endothelial cells. *Circ Res*. 1998;82:619–628.

Investigative Ophthalmology & Visual Science